3 Basic concepts for two-dimensional NMR

3.1 Introduction

The basic ideas of two-dimensional NMR will be introduced by reference to the appearance of a COSY spectrum; later in this lecture the product operator formalism will be used to predict the form of the spectrum.

Conventional NMR spectra (one-dimensional spectra) are plots of intensity *vs.* frequency; in two-dimensional spectroscopy intensity is plotted as a function of two frequencies, usually called F_1 and F_2. There are various ways of representing such a spectrum on paper, but the one most usually used is to make a contour plot in which the intensity of the peaks is represented by contour lines drawn at suitable intervals, in the same way as a topographical map. The position of each peak is specified by two frequency co-ordinates corresponding to F_1 and F_2. Two-dimensional NMR spectra are always arranged so that the F_2 co-ordinates of the peaks correspond to those found in the normal one-dimensional spectrum, and this relation is often emphasized by plotting the one-dimensional spectrum alongside the F_2 axis.

The figure shows a schematic COSY spectrum of a hypothetical molecule containing just two protons, A and X, which are coupled together. The one-dimensional spectrum is plotted alongside the F_2 axis, and consists of the familiar pair of doublets centred on the chemical shifts of A and X, δ_A and δ_X respectively. In the COSY spectrum, the F_1 co-ordinates of the peaks in the two-dimensional spectrum also correspond to those found in the normal one-dimensional spectrum and to emphasize this point the one-dimensional spectrum has been plotted alongside the F_1 axis. It is immediately clear that this COSY spectrum has some symmetry about the diagonal $F_1 = F_2$ which has been indicated with a dashed line.

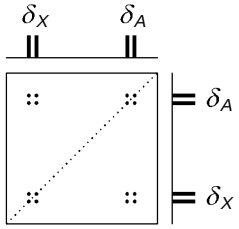

Schematic COSY spectrum for two coupled spins, A and X

In a one-dimensional spectrum scalar couplings give rise to multiplets in the spectrum. In two-dimensional spectra the idea of a multiplet has to be expanded somewhat so that in such spectra a multiplet consists of an array of individual peaks often giving the impression of a square or rectangular outline. Several such arrays of peaks can be seen in the schematic COSY spectrum shown above. These two-dimensional multiplets come in two distinct types: diagonal-peak multiplets which are centred around the same F_1 and F_2 frequency co-ordinates and cross-peak multiplets which are centred around different F_1 and F_2 co-ordinates. Thus in the schematic COSY spectrum there are two diagonal-peak multiplets centred at $F_1 = F_2 = \delta_A$ and $F_1 = F_2 = \delta_X$, one cross-peak multiplet centred at $F_1 = \delta_A$, $F_2 = \delta_X$ and a second cross-peak multiplet centred at $F_1 = \delta_X$, $F_2 = \delta_A$.

The appearance in a COSY spectrum of a cross-peak multiplet $F_1 = \delta_A$, $F_2 = \delta_X$ indicates that the two protons at shifts δ_A and δ_X have a scalar coupling between them. This statement is all that is required for the analysis of a COSY spectrum, and it is this simplicity which is the key to the great utility of such spectra. From a single COSY spectrum it is possible to trace out the whole coupling network in the molecule.

3.1.1 General Scheme for two-Dimensional NMR

In one-dimensional pulsed Fourier transform NMR the signal is recorded as a function of one time variable and then Fourier transformed to give a spectrum which is a function of one frequency variable. In two-dimensional NMR the signal is recorded as a function of two time variables, t_1 and t_2, and the resulting data Fourier transformed twice to yield a spectrum which is a function of two frequency variables. The general scheme for two-dimensional spectroscopy is

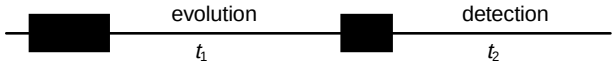

In the first period, called the preparation time, the sample is excited by one or more pulses. The resulting magnetization is allowed to evolve for the first time period, t_1. Then another period follows, called the mixing time, which consists of a further pulse or pulses. After the mixing period the signal is recorded as a function of the second time variable, t_2. This sequence of events is called a pulse sequence and the exact nature of the preparation and mixing periods determines the information found in the spectrum.

It is important to realize that the signal is not recorded during the time t_1, but only during the time t_2 at the end of the sequence. The data is recorded at regularly spaced intervals in both t_1 and t_2.

The two-dimensional signal is recorded in the following way. First, t_1 is set to zero, the pulse sequence is executed and the resulting free induction decay recorded. Then the nuclear spins are allowed to return to equilibrium. t_1 is then set to Δ_1, the sampling interval in t_1, the sequence is repeated and a free induction decay is recorded and stored separately from the first. Again the spins are allowed to equilibrate, t_1 is set to $2\Delta_1$, the pulse sequence repeated and a free induction decay recorded and stored. The whole process is repeated again for $t_1 = 3\Delta_1$, $4\Delta_1$ and so on until sufficient data is recorded, typically 50 to 500 increments of t_1. Thus recording a two-dimensional data set involves repeating a pulse sequence for increasing values of t_1 and recording a free induction decay as a function of t_2 for each value of t_1.

3.1.2 Interpretation of peaks in a two-dimensional spectrum

Within the general framework outlined in the previous section it is now possible to interpret the appearance of a peak in a two-dimensional spectrum at particular frequency co-ordinates.

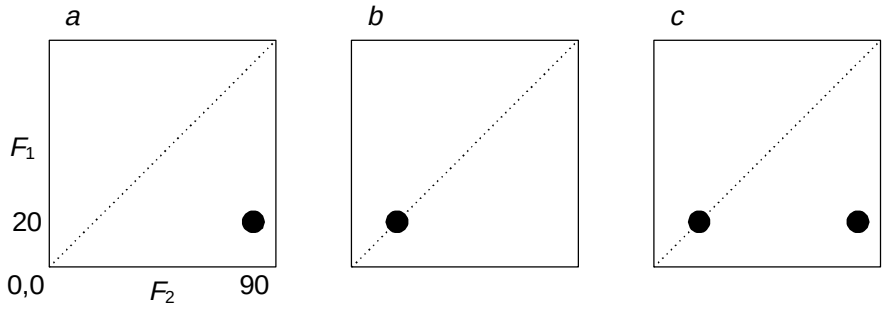

Suppose that in some unspecified two-dimensional spectrum a peak appears at F_1 = 20 Hz, F_2 = 90 Hz (spectrum *a* above) The interpretation of this peak is that a signal was present during t_1 which evolved with a frequency of 20 Hz. During the mixing time this *same* signal was transferred in some way to another signal which evolved at 90 Hz during t_2.

Likewise, if there is a peak at F_1 = 20 Hz, F_2 = 20 Hz (spectrum *b*) the interpretation is that there was a signal evolving at 20 Hz during t_1 which was unaffected by the mixing period and continued to evolve at 20 Hz during t_2. The processes by which these signals are transferred will be discussed in the following sections.

Finally, consider the spectrum shown in *c*. Here there are two peaks, one at F_1 = 20 Hz, F_2 = 90 Hz and one at F_1 = 20 Hz, F_2 = 20 Hz. The interpretation of this is that some signal was present during t_1 which evolved at 20 Hz and that during the mixing period part of it was transferred into another signal which evolved at 90 Hz during t_2. The other part remained unaffected and continued to evolve at 20 Hz. On the basis of the previous discussion of COSY spectra, the part that changes frequency during the mixing time is recognized as leading to a cross-peak and the part that does not change frequency leads to a diagonal-peak. This kind of interpretation is a very useful way of thinking about the origin of peaks in a two-dimensional spectrum.

It is clear from the discussion in this section that the mixing time plays a crucial role in forming the two-dimensional spectrum. In the absence of a mixing time, the frequencies that evolve during t_1 and t_2 would be the same and only diagonal-peaks would appear in the spectrum. To obtain an interesting and useful spectrum it is essential to arrange for some process during the mixing time to transfer signals from one spin to another.

3.2 EXSY and NOESY spectra in detail

In this section the way in which the EXSY (EXchange SpectroscopY) sequence works will be examined; the pulse sequence is shown opposite. This experiment gives a spectrum in which a cross-peak at frequency co-ordinates $F_1 = \delta_A$, $F_2 = \delta_B$ indicates that the spin resonating at δ_A is chemically exchanging with the spin resonating at δ_B.

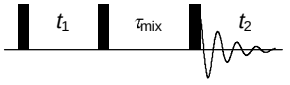

The pulse sequence for EXSY (and NOESY). All pulses have 90° flip angles.

The pulse sequence for EXSY is shown opposite. The effect of the sequence will be analysed for the case of two spins, 1 and 2, but without any coupling between them. The initial state, before the first pulse, is equilibrium magnetization, represented as $I_{1z} + I_{2z}$; however, for simplicity only magnetization from the first spin will be considered in the calculation.

The first 90° pulse (of phase *x*) rotates the magnetization onto –*y*

$$I_{1z} \xrightarrow{\pi/2\, I_{1x}} \xrightarrow{\pi/2\, I_{2x}} -I_{1y}$$

(the second arrow has no effect as it involves operators of spin 2). Next follows evolution for time t_1

$$-I_{1y} \xrightarrow{\Omega_1 t_1\, I_{1z}} \xrightarrow{\Omega_2 t_1\, I_{2z}} -\cos\Omega_1 t_1\ I_{1y} + \sin\Omega_1 t_1\ I_{1x}$$

again, the second arrow has no effect. The second 90° pulse turns the first term onto the *z*-axis and leaves the second term unaffected

$$-\cos\Omega_1 t_1\ I_{1y} \xrightarrow{\pi/2\, I_{1x}} \xrightarrow{\pi/2\, I_{2x}} -\cos\Omega_1 t_1\ I_{1z}$$
$$\sin\Omega_1 t_1\ I_{1x} \xrightarrow{\pi/2\, I_{1x}} \xrightarrow{\pi/2\, I_{2x}} \sin\Omega_1 t_1\ I_{1x}$$

Only the I_{1z} term leads to cross-peaks by chemical exchange, so the other term will be ignored (in an experiment this is achieved by appropriate coherence pathway selection – see lecture 4). The effect of the first part of the sequence is to generate, at the start of the mixing time, τ_{mix}, some *z*-magnetization on spin 1 whose size depends, via the cosine term, on t_1 and the frequency, Ω_1, with which the spin 1 evolves during t_1. The magnetization is said to be frequency labelled.

During the mixing time, τ_{mix}, spin 1 may undergo chemical exchange with spin 2. If it does this, it carries with it the frequency label that it acquired during t_1. The extent to which this transfer takes place depends on the details of the chemical kinetics; it will be assumed simply that during τ_{mix} a fraction *f* of the spins of type 1 chemically exchange with spins of type 2. The effect of the mixing process can then be written

$$-\cos\Omega_1 t_1\ I_{1z} \xrightarrow{\text{mixing}} -(1-f)\cos\Omega_1 t_1\ I_{1z} - f\cos\Omega_1 t_1\ I_{2z}$$

The final 90° pulse rotates this *z*-magnetization back onto the *y*-axis

$$-(1-f)\cos\Omega_1 t_1\ I_{1z} \xrightarrow{\pi/2\, I_{1x}} \xrightarrow{\pi/2\, I_{2x}} (1-f)\cos\Omega_1 t_1\ I_{1y}$$
$$-f\cos\Omega_1 t_1\ I_{2z} \xrightarrow{\pi/2\, I_{1x}} \xrightarrow{\pi/2\, I_{2x}} f\cos\Omega_1 t_1\ I_{2y}$$

Although the magnetization started on spin 1, at the end of the sequence there is magnetization present on spin 2 – a process called magnetization transfer. The analysis of the experiment is completed by allowing the I_{1y} and I_{2y} operators to evolve for time t_2.

$$(1-f)\cos\Omega_1 t_1\ I_{1y} \xrightarrow{\Omega_1 t_2\ I_{1z}} \xrightarrow{\Omega_2 t_2\ I_{2z}}$$
$$(1-f)\cos\Omega_1 t_2 \cos\Omega_1 t_1\ I_{1y} - (1-f)\sin\Omega_1 t_2 \cos\Omega_1 t_1\ I_{1x}$$
$$f\cos\Omega_1 t_1\ I_{2y} \xrightarrow{\Omega_1 t_2\ I_{1z}} \xrightarrow{\Omega_2 t_2\ I_{2z}}$$
$$f\cos\Omega_2 t_2 \cos\Omega_1 t_1\ I_{2y} - f\sin\Omega_2 t_2 \cos\Omega_1 t_1\ I_{2x}$$

If it is assumed that the *y*-magnetization is detected during t_2 (this is an arbitrary choice, but a convenient one), the time domain signal has two terms:

$$(1-f)\cos\Omega_1 t_2 \cos\Omega_1 t_1 + f\cos\Omega_2 t_2 \cos\Omega_1 t_1$$

The crucial thing is that the amplitude of the signal recorded during t_2 is modulated by the evolution during t_1. This can be seen more clearly by imagining the Fourier transform, with respect to t_2, of the above function. The $\cos(\Omega_1 t_2)$ and $\cos(\Omega_2 t_2)$ terms transform to give absorption mode signals centred at Ω_1 and Ω_2 respectively in the F_2 dimension; these are denoted $A_1^{(2)}$ and $A_2^{(2)}$ (the subscript indicates which spin, and the superscript which dimension). The time domain function becomes

$$(1-f)A_1^{(2)}\cos\Omega_1 t_1 + fA_2^{(2)}\cos\Omega_1 t_1$$

If a series of spectra recorded as t_1 progressively increases are inspected it would be found that the $\cos(\Omega_1 t_2)$ term causes a change in size of the peaks at Ω_1 and Ω_2 – this is the modulation referred to above.

Fourier transformation with respect to t_1 gives peaks with an absorption lineshape, but this time in the F_1 dimension; an absorption mode signal at Ω_1 in F_1 is denoted $A_1^{(1)}$. The time domain signal becomes, after Fourier transformation in each dimension

$$(1-f)A_2^{(1)}A_1^{(1)} + fA_2^{(2)}A_1^{(1)}$$

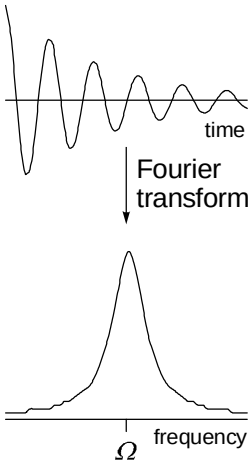

The Fourier transform of a decaying cosine function $\cos\Omega t \exp(-t/T_2)$ is an absorption mode Lorentzian centred at frequency Ω.

Thus, the final two-dimensional spectrum is predicted to have two peaks. One is at $(F_1, F_2) = (\Omega_1, \Omega_1)$ – this is a diagonal peak and arises from those spins of type 1 which did not undergo chemical exchange during τ_{mix}. The second is at $(F_1, F_2) = (\Omega_1, \Omega_2)$ – this is a cross peak which indicates that part of the magnetization from spin 1 was transferred to spin 2 during the mixing time. It is this peak that contains the useful information. If the calculation were repeated starting with magnetization on spin 2 it would be found that there are similar peaks at (Ω_2, Ω_2) and (Ω_2, Ω_1).

The NOESY (Nuclear Overhauser Effect SpectrocopY) spectrum is recorded using the same basic sequence. The only difference is that during the mixing time the cross-relaxation is responsible for the exchange of magnetization between different spins. Thus, a cross-peak indicates that two spins are experiencing mutual cross-relaxation and hence are close in space.

Having completed the analysis it can now be seen how the EXCSY/NOESY sequence is put together. First, the $90° - t_1 - 90°$ sequence is used to generate frequency labelled *z*-magnetization. Then, during τ_{mix}, this magnetization is allowed to migrate to other spins, carrying its label with it. Finally, the last pulse renders the *z*-magnetization observable.

3.3 More about two-dimensional transforms

From the above analysis it was seen that the signal observed during t_2 has an amplitude proportional to $\cos(\Omega_1 t_1)$; the amplitude of the signal observed during t_2 depends on the evolution during t_1. For the first increment of t_1 ($t_1 = 0$), the signal will be a maximum, the second increment will have size proportional to $\cos(\Omega_1 \Delta_1)$, the third proportional to $\cos(\Omega_1 2\Delta_1)$, the fourth to $\cos(\Omega_1 3\Delta_1)$ and so on. This modulation of the amplitude of the observed signal by the t_1 evolution is illustrated in the figure below.

In the figure the first column shows a series of free induction decays that would be recorded for increasing values of t_1 and the second column shows the Fourier transforms of these signals. The final step in constructing the two-dimensional spectrum is to Fourier transform the data along the t_1 dimension. This process is also illustrated in the figure. Each of the spectra shown in the second column are represented as a series of data points, where each point corresponds to a different F_2 frequency. The data point corresponding to a particular F_2 frequency is selected from the spectra for $t_1 = $, $t_1 = \Delta_1$, $t_1 = 2\Delta_1$ and so on for all the t_1 values. Such a process results in a function, called an interferogram, which has t_1 as the running variable.

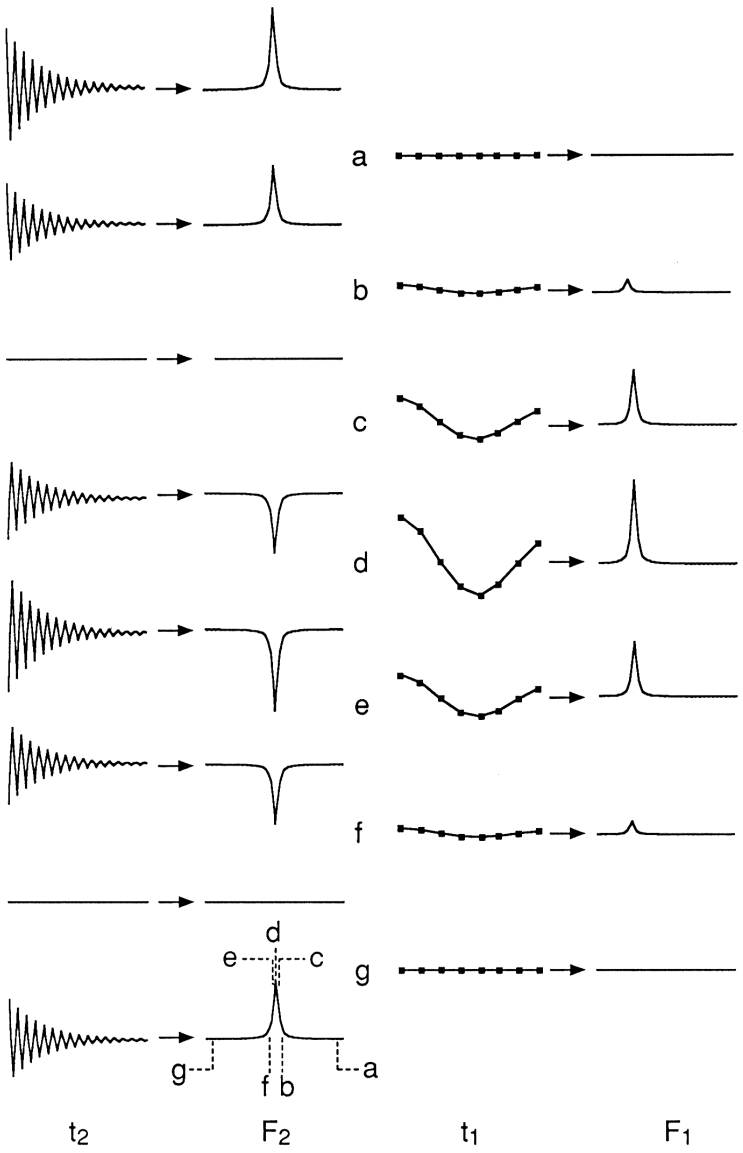

Illustration of how the modulation of a free induction decay by evolution during t_1 gives rise to a peak in the two-dimensional spectrum. In the left most column is shown a series of free induction decays that would be recorded for successive values of t_1; t_1 increases down the page. Note how the amplitude of these free induction decays varies with t_1, something that becomes even plainer when the time domain signals are Fourier transformed, as shown in the second column. In practice, each of these F_2 spectra in column two consist of a series of data points. The data point at the same frequency in each of these spectra is extracted and assembled into an interferogram, in which the horizontal axis is the time t_1. Several such interferograms, labelled *a* to *g*, are shown in the third column. Note that as there were eight F_2 spectra in column two corresponding to different t_1 values there are eight points in each interferogram. The F_2 frequencies at which the interferograms are taken are indicated on the lower spectrum of the second column. Finally, a second Fourier transformation of these interferograms gives a series of F_1 spectra shown in the right hand column. Note that in this column F_2 increases down the page, whereas in the first column t_1 increase down the page. The final result is a two-dimensional spectrum containing a single peak.

Several interferograms, labelled *a* to *g*, computed for different F_2 frequencies are shown in the third column of the figure. The particular F_2 frequency that each interferogram corresponds to is indicated in the bottom spectrum of the second column. The amplitude of the signal in each interferogram is different, but in this case the modulation frequency is the same. The final stage in the processing is to Fourier transform these interferograms to give the series of spectra which are shown in the right most column of the figure. These spectra have F_1 running horizontally and

F_2 running down the page. The modulation of the time domain signal has been transformed into a single two-dimensional peak. Note that the peak appears on several traces corresponding to different F_2 frequencies because of the width of the line in F_2.

The time domain data in the t_1 dimension can be manipulated by multiplying by weighting functions or zero filling, just as with conventional free induction decays.

3.4 Two-dimensional experiments using coherence transfer through *J*-coupling

Perhaps the most important set of two-dimensional experiments are those which transfer magnetization from one spin to another via the scalar coupling between them. As was seen in section 2.3.3, this kind of transfer can be brought about by the action of a pulse on an anti-phase state. In outline the basic process is

$$I_{1x} \xrightarrow{\text{coupling}} 2I_{1y}I_{2z} \xrightarrow{90°(x)\text{ to both spins}} 2I_{1z}I_{2y}$$
$$\text{spin 1} \qquad\qquad \text{spin 2}$$

3.4.1 COSY

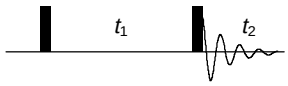

Pulse sequence for the two-dimensional COSY experiment

The pulse sequence for this experiment is shown opposite. It will be assumed in the analysis that all of the pulses are applied about the *x*-axis and for simplicity the calculation will start with equilibrium magnetization only on spin 1. The effect of the first pulse is to generate *y*-magnetization, as has been worked out previously many times

$$I_{1z} \xrightarrow{\pi/2 I_{1x}} \xrightarrow{\pi/2 I_{2x}} -I_{1y}$$

This state then evolves for time t_1, first under the influence of the offset of spin 1 (that of spin 2 has no effect on spin 1 operators):

$$-I_{1y} \xrightarrow{\Omega_1 t_1 I_{1z}} -\cos\Omega_1 t_1\, I_{1y} + \sin\Omega_1 t_1\, I_{1x}$$

Both terms on the right then evolve under the coupling

$$-\cos\Omega_1 t_1\, I_{1y} \xrightarrow{2\pi J_{12} t_1 I_{1z} I_{2z}} -\cos\pi J_{12} t_1 \cos\Omega_1 t_1\, I_{1y} + \sin\pi J_{12} t_1 \cos\Omega_1 t_1\, 2I_{1x}I_{2z}$$
$$\sin\Omega_1 t_1\, I_{1x} \xrightarrow{2\pi J_{12} t_1 I_{1z} I_{2z}} \cos\pi J_{12} t_1 \sin\Omega_1 t_1\, I_{1x} + \sin\pi J_{12} t_1 \sin\Omega_1 t_1\, 2I_{1y}I_{2z}$$

That completes the evolution under t_1. Now all that remains is to consider the effect of the final pulse, remembering that the effect of the pulse on both spins needs to be computed. Taking the terms one by one:

$$-\cos\pi J_{12}t_1\cos\Omega_1 t_1\ I_{1y} \xrightarrow{\pi/2I_{1x}} \xrightarrow{\pi/2I_{2x}} -\cos\pi J_{12}t_1\cos\Omega_1 t_1\ I_{1z} \quad \{1\}$$

$$\sin\pi J_{12}t_1\cos\Omega_1 t_1\ 2I_{1x}I_{2z} \xrightarrow{\pi/2I_{1x}} \xrightarrow{\pi/2I_{2x}} -\sin\pi J_{12}t_1\cos\Omega_1 t_1\ 2I_{1x}I_{2y} \quad \{2\}$$

$$\cos\pi J_{12}t_1\sin\Omega_1 t_1\ I_{1x} \xrightarrow{\pi/2I_{1x}} \xrightarrow{\pi/2I_{2x}} \cos\pi J_{12}t_1\sin\Omega_1 t_1\ I_{1x} \quad \{3\}$$

$$\sin\pi J_{12}t_1\sin\Omega_1 t_1\ 2I_{1y}I_{2z} \xrightarrow{\pi/2I_{1x}} \xrightarrow{\pi/2I_{2x}} -\sin\pi J_{12}t_1\sin\Omega_1 t_1\ 2I_{1z}I_{2y} \quad \{4\}$$

Terms {1} and {2} are unobservable. Term {3} corresponds to in-phase magnetization of spin 1, aligned along the *x*-axis. The t_1 modulation of this term depends on the offset of spin 1, so a diagonal peak centred at (Ω_1,Ω_1) is predicted. Term {4} is the really interesting one. It shows that anti-phase magnetization on spin 1, $2I_{1y}I_{2z}$, is transferred to anti-phase magnetization on spin 2, $2I_{1z}I_{2y}$; this is an example of coherence transfer. Term {4} appears as observable magnetization on spin 2, but it is modulated in t_1 with the offset of spin 1, thus it gives rise to a cross-peak centred at (Ω_1,Ω_2). It has been shown, therefore, how cross- and diagonal-peaks arise in a COSY spectrum.

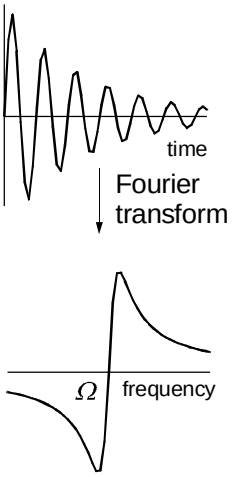

The Fourier transform of a decaying sine function $\sin\Omega t\ \exp(-t/T_2)$ is a dispersion mode Lorentzian centred at frequency Ω.

Some more consideration should be give to the form of the cross- and diagonal peaks. Consider again term {3}: it will give rise to an in-phase multiplet in F_2, and as it is along the *x*-axis, the lineshape will be dispersive. The form of the modulation in t_1 can be expanded, using the formula, $\cos A\sin B = \frac{1}{2}\{\sin(B+A)+\sin(B-A)\}$ to give

$$\cos\pi J_{12}t_1\sin\Omega_1 t_1 = \tfrac{1}{2}\left\{\sin\left(\Omega_1 t_1+\pi J_{12}t_1\right)+\sin\left(\Omega_1 t_1-\pi J_{12}t\right)\right\}$$

Two peaks in F_1 are expected at $\Omega_1 \pm \pi J_{12}$, these are just the two lines of the spin 1 doublet. In addition, since these are sine modulated they will have the dispersion lineshape. Note that both components in the spin 1 multiplet observed in F_2 are modulated in this way, so the appearance of the two-dimensional multiplet can best be found by "multiplying together" the multiplets in the two dimensions, as shown opposite. In addition, all four components of the diagonal-peak multiplet have the same sign, and have the double dispersion lineshape illustrated below

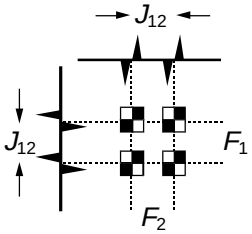

Schematic view of the diagonal peak from a COSY spectrum. The squares are supposed to indicate the two-dimensional double dispersion lineshape illustrated below

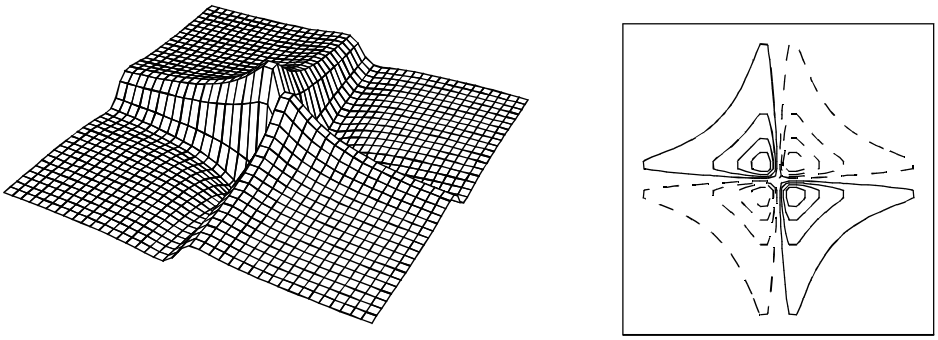

The double dispersion lineshape seen in pseudo 3D and as a contour plot; negative contours are indicated by dashed lines.

Term {4} can be treated in the same way. In F_2 we know that this term

gives rise to an anti-phase absorption multiplet on spin 2. Using the relationship $\sin B \sin A = \frac{1}{2}\{-\cos(B+A) + \cos(B-A)\}$ the modulation in t_1 can be expanded

$$\sin \pi J_{12} t_1 \sin \Omega_1 t = \tfrac{1}{2}\left\{-\cos\left(\Omega_1 t_1 + \pi J_{12} t_1\right) + \cos\left(\Omega_1 t_1 - \pi J_{12} t\right)\right\}$$

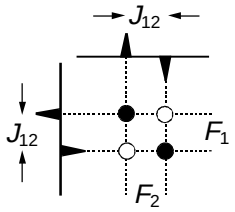

Schematic view of the cross-peak multiplet from a COSY spectrum. The circles are supposed to indicate the two-dimensional double absorption lineshape illustrated below; filled circles represent positive intensity, open represent negative intensity.

Two peaks in F_1, at $\Omega_1 \pm \pi J_{12}$, are expected; these are just the two lines of the spin 1 doublet. Note that the two peaks have opposite signs – that is they are anti-phase in F_1. In addition, since these are cosine modulated we expect the absorption lineshape (see section 3.2). The form of the cross-peak multiplet can be predicted by "multiplying together" the F_1 and F_2 multiplets, just as was done for the diagonal-peak multiplet. The result is shown opposite. This characteristic pattern of positive and negative peaks that constitutes the cross-peak is know as an anti-phase square array.

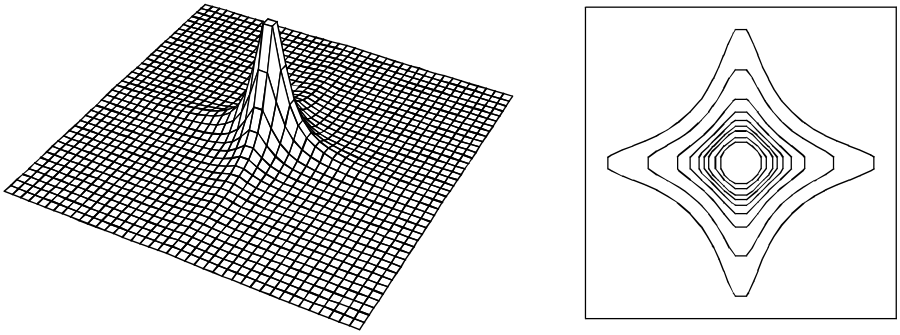

The double absorption lineshape seen in pseudo 3D and as a contour plot.

COSY spectra are sometimes plotted in the absolute value mode, where all the sign information is suppressed deliberately. Although such a display is convenient, especially for routine applications, it is generally much more desirable to retain the sign information. Spectra displayed in this way are said to be phase sensitive; more details of this are given in section 3.6.

As the coupling constant becomes comparable with the linewidth, the positive and negative peaks in the cross-peak multiplet begin to overlap and cancel one another out. This leads to an overall reduction in the intensity of the cross-peak multiplet, and ultimately the cross-peak disappears into the noise in the spectrum. The smallest coupling which gives rise to a cross-peak is thus set by the linewidth and the signal-to-noise ratio of the spectrum.

3.4.2 Double-quantum filtered COSY (DQF COSY)

The conventional COSY experiment suffers from a disadvantage which arises from the different phase properties of the cross- and diagonal-peak multiplets. The components of a diagonal peak multiplet are all in-phase and so tend to reinforce one another. In addition, the dispersive tails of these peaks spread far into the spectrum. The result is a broad intense diagonal which can obscure nearby cross-peaks. This effect is particularly troublesome when the coupling is comparable with the linewidth as in such

cases, as was described above, cancellation of anti-phase components in the cross-peak multiplet reduces the overall intensity of these multiplets.

This difficulty is neatly side-stepped by a modification called double quantum filtered COSY (DQF COSY). The pulse sequence is shown opposite.

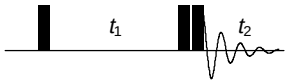

The pulse sequence for DQF COSY; the delay between the last two pulses is usually just a few microseconds.

Up to the second pulse the sequence is the same as COSY. However, it is arranged that only double-quantum coherence present during the (very short) delay between the second and third pulses is ultimately allowed to contribute to the spectrum. Hence the name, "double-quantum filtered", as all the observed signals are filtered through double-quantum coherence. The final pulse is needed to convert the double quantum coherence back into observable magnetization. This double-quantum derived signal is selected by the use of coherence pathway selection using phase cycling or field gradient pulses, further details of which will be given in lecture 4.

In the analysis of the COSY experiment, it is seen that after the second 90° pulse it is term {2} that contains double-quantum coherence; this can be demonstrated explicitly by expanding this term in the raising and lowering operators, as was done in section 2.5

$$\begin{aligned} 2I_{1x}I_{2y} &= 2\times\tfrac{1}{2}\left(I_{1+}+I_{1-}\right)\times\tfrac{1}{2i}\left(I_{2+}-I_{2-}\right) \\ &= \tfrac{1}{2i}\left(I_{1+}I_{2+}-I_{1-}I_{2-}\right)+\tfrac{1}{2i}\left(-I_{1+}I_{2-}+I_{1-}I_{2+}\right) \end{aligned}$$

This term contains both double- and zero-quantum coherence. The pure double-quantum part is the term in the first bracket on the right; this term can be re-expressed in Cartesian operators:

$$\begin{aligned} \tfrac{1}{2i}\left(I_{1+}I_{2+}-I_{1-}I_{2-}\right) &= \tfrac{1}{2i}\left[\left(I_{1x}+iI_{1y}\right)\left(I_{1x}+iI_{1y}\right)+\left(I_{2x}-iI_{2y}\right)\left(I_{2x}-iI_{2y}\right)\right] \\ &= \tfrac{1}{2}\left[2I_{1x}I_{2y}+2I_{1y}I_{2x}\right] \end{aligned}$$

The effect of the last 90°(*x*) pulse on the double quantum part of term {2} is thus

$$-\tfrac{1}{2}\sin\pi J_{12}t_1\cos\Omega_1 t_1\left(2I_{1x}I_{2y}+2I_{1y}I_{2x}\right)\xrightarrow{\pi/2I_{1x}}\xrightarrow{\pi/2I_{2x}} -\tfrac{1}{2}\sin\pi J_{12}t_1\cos\Omega_1 t_1\left(2I_{1x}I_{2z}+2I_{1z}I_{2x}\right)$$

The first term on the right is anti-phase magnetization of spin 1 aligned along the *x*-axis; this gives rise to a diagonal-peak multiplet. The second term is anti-phase magnetization of spin 2, again aligned along *x*; this will give rise to a cross-peak multiplet. Both of these terms have the same modulation in t_1, which can be shown, by a similar analysis to that used above, to lead to an anti-phase multiplet in F_1. As these peaks all have the same lineshape the overall phase of the spectrum can be adjusted so that they are all in absorption; see section 3.6 for further details. In contrast to the case of a simple COSY experiment both the diagonal- and cross-peak multiplets are in anti-phase in both dimensions, thus avoiding the strong in-

phase diagonal peaks found in the simple experiment. The DQF COSY experiment is the method of choice for tracing out coupling networks in a molecule.

3.4.3 Heteronuclear correlation experiments

One particularly useful experiment is to record a two-dimensional spectrum in which the co-ordinate of a peak in one dimension is the chemical shift of one type of nucleus (e.g. proton) and the co-ordinate in the other dimension is the chemical shift of another nucleus (e.g. carbon-13) which is coupled to the first nucleus. Such spectra are often called shift correlation maps or shift correlation spectra.

The one-bond coupling between a carbon-13 and the proton directly attached to it is relatively constant (around 150 Hz), and much larger than any of the long-range carbon-13 proton couplings. By utilizing this large difference experiments can be devised which give maps of carbon-13 shifts *vs* the shifts of directly attached protons. Such spectra are very useful as aids to assignment; for example, if the proton spectrum has already been assigned, simply recording a carbon-13 proton correlation experiment will give the assignment of all the protonated carbons.

Only one kind of nuclear species can be observed at a time, so there is a choice as to whether to observe carbon-13 or proton when recording a shift correlation spectrum. For two reasons, it is very advantageous from the sensitivity point of view to record protons. First, the proton magnetization is larger than that of carbon-13 because there is a larger separation between the spin energy levels giving, by the Boltzmann distribution, a greater population difference. Second, a given magnetization induces a larger voltage in the coil the higher the NMR frequency becomes.

Trying to record a carbon-13 proton shift correlation spectrum by proton observation has one serious difficulty. Carbon-13 has a natural abundance of only 1%, thus 99% of the molecules in the sample do not have any carbon-13 in them and so will not give signals that can be used to correlate carbon-13 and proton. The 1% of molecules with carbon-13 will give a perfectly satisfactory spectrum, but the signals from these resonances will be swamped by the much stronger signals from non-carbon-13 containing molecules. However, these unwanted signals can be suppressed using coherence selection in a way which will be described below and which will be further elaborated in lecture 4.

3.4.3.1 Heteronuclear multiple-quantum correlation (HMQC)

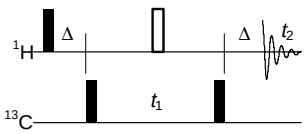

The pulse sequence for HMQC. Filled rectangles represent 90° pulses and open rectangles represent 180° pulses. The delay Δ is set to $1/(2J_{12})$.

The pulse sequence for this popular experiment is given opposite. The sequence will be analysed for a coupled carbon-13 proton pair, where spin 1 will be the carbon-13 and spin 2 the proton.

The analysis will start with equilibrium magnetization on spin 1, I_{1z}. The whole analysis can be greatly simplified by noting that the 180° pulse is exactly midway between the first 90° pulse and the start of data acquisition. As has been shown in section 2.4, such a sequence forms a spin echo and so the evolution of the offset of spin 1 over the entire period (t_1 + 2Δ) is refocused. Thus the evolution of the offset of spin 1 can simply be ignored

for the purposes of the calculation.

At the end of the delay Δ the state of the system is simply due to evolution of the term $-I_{1y}$ under the influence of the scalar coupling:

$$-\cos\pi J_{12}\Delta\ I_{1y} + \sin\pi J_{12}\Delta\ 2I_{1x}I_{2z}$$

It will be assumed that $\Delta = 1/(2J_{12})$, so only the anti-phase term is present.

The second 90° pulse is applied to carbon-13 (spin 2) only

$$2I_{1x}I_{2z} \xrightarrow{\pi/2\,I_{2x}} -2I_{1x}I_{2y}$$

This pulse generates a mixture of heteronuclear double- and zero-quantum coherence, which then evolves during t_1. In principle this term evolves under the influence of the offsets of spins 1 and 2 and the coupling between them. However, it has already been noted that the offset of spin 1 is refocused by the centrally placed 180° pulse, so it is not necessary to consider evolution due to this term. In addition, it can be shown that multiple-quantum coherence involving spins i and j does not evolve under the influence of the coupling, J_{ij}, between these two spins (see appendix x.x). As a result of these two simplifications, the only evolution that needs to be considered is that due to the offset of spin 2 (the carbon-13).

$$-2I_{1x}I_{2y} \xrightarrow{\Omega_2 t_1 I_{2z}} -\cos\Omega_2 t_1\ 2I_{1x}I_{2y} + \sin\Omega_2 t_1\ 2I_{1x}I_{2x}$$

The second 90° pulse to spin 2 (carbon-13) regenerates the first term on the right into spin 1 (proton) observable magnetization; the other remains unobservable

$$-\cos\Omega_2 t_1\ 2I_{1x}I_{2y} \xrightarrow{\pi/2\,I_{2x}} -\cos\Omega_2 t_1\ 2I_{1x}I_{2z}$$

This term then evolves under the coupling, again it is assumed that $\Delta = 1/(2J_{12})$

$$-\cos\Omega_2 t_1\ 2I_{1x}I_{2z} \xrightarrow{2\pi J_{12}\Delta I_{1z}I_{2z},\ \Delta=1/(2J_{12})} -\cos\Omega_2 t_1\ I_{1y}$$

This is a very nice result; in F_2 there will be an in-phase doublet centred at the offset of spin 1 (proton) and these two peaks will have an F_1 co-ordinate simply determined by the offset of spin 2 (carbon-13); the peaks will be in absorption. A schematic spectrum is shown opposite.

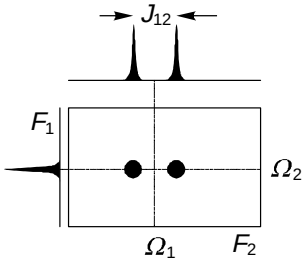

Schematic HMQC spectrum for two coupled spins.

The problem of how to suppress the very strong signals from protons not coupled to any carbon-13 nuclei now has to be addressed. From the point of view of these protons the carbon-13 pulses might as well not even be there, and the pulse sequence looks like a simple spin echo. This insensitivity to the carbon-13 pulses is the key to suppressing the unwanted signals.

Suppose that the phase of the first carbon-13 90° pulse is altered from *x* to –*x*. Working through the above calculation it is found that the wanted signal from the protons coupled to carbon-13 changes sign i.e. the observed spectrum will be inverted. In contrast the signal from a proton not coupled to carbon-13 will be unaffected by this change. Thus, for each t_1 increment the free induction decay is recorded twice: once with the first carbon-13 90° pulse set to phase *x* and once with it set to phase –*x*. The two free induction decays are then subtracted in the computer memory thus cancelling the unwanted signals. This is an example of a very simple phase cycle, more details of which are given in lecture 4.

In the case of carbon-13 and proton the one bond coupling is so much larger than any of the long range couplings that a choice of $\Delta = 1/(2J_{\text{one bond}})$ does not give any correlations other than those through the one-bond coupling. There is simply insufficient time for the long-range couplings to become anti-phase. However, if Δ is set to a much longer value (30 to 60 ms), long-range correlations will be seen. Such spectra are very useful in assigning the resonances due to quaternary carbon-13 atoms. The experiment is often called HMBC (heteronuclear multiple-bond correlation).

Now that the analysis has been completed it can be seen what the function of various elements in the pulse sequence is. The first pulse and delay generate magnetization on proton which is anti-phase with respect to the coupling to carbon-13. The carbon-13 90° pulse turns this into multiple quantum coherence. This forms a filter through which magnetization not bound to carbon-13 cannot pass and it is the basis of discrimination between signals from protons bound and not bound to carbon-13. The second carbon-13 pulse returns the multiple quantum coherence to observable anti-phase magnetization on proton. Finally, the second delay Δ turns the anti-phase state into an in-phase state. The centrally placed proton 180° pulse refocuses the proton shift evolution for both the delays Δ and t_1.

3.4.3.2 Heteronuclear single-quantum correlation (HSQC)

This pulse sequence results in a spectrum identical to that found for HMQC. Despite the pulse sequence being a little more complex than that for HMQC, HSQC has certain advantages for recording the spectra of large molecules, such a proteins. The HSQC pulse sequence is often embedded in much more complex sequences which are used to record two- and three-dimensional spectra of carbon-13 and nitrogen-15 labelled proteins.

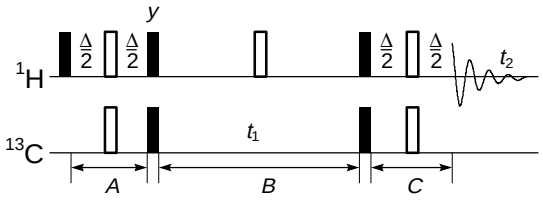

The pulse sequence for HSQC. Filled rectangles represent 90° pulses and open rectangles represent 180° pulses. The delay Δ is set to $1/(2J_{12})$; all pulses have phase x unless otherwise indicated.

If this sequence were to be analysed by considering each delay and pulse in turn the resulting calculation would be far too complex to be useful. A more intelligent approach is needed where simplifications are used, for example

by recognizing the presence of spin echoes who refocus offsets or couplings. Also, it is often the case that attention can be focused a particular terms, as these are the ones which will ultimately lead to observable signals. This kind of "intelligent" analysis will be illustrated here.

Periods *A* and *C* are spin echoes in which 180° pulses are applied to both spins; it therefore follows that the offsets of spins 1 and 2 will be refocused, but the coupling between them will evolve throughout the entire period. As the total delay in the spin echo is $1/(2J_{12})$ the result will be the complete conversion of in-phase into anti-phase magnetization.

Period *B* is a spin echo in which a 180° pulse is applied only to spin 1. Thus, the offset of spin 1 is refocused, as is the coupling between spins 1 and 2; only the offset of spin 2 affects the evolution.

With these simplifications the analysis is easy. The first pulse generates $-I_{1y}$; during period *A* this then becomes $-2I_{1x}I_{2z}$. The 90°(*y*) pulse to spin 1 turns this to $2I_{1z}I_{2z}$ and the 90°(*x*) pulse to spin 2 turns it to $-2I_{1z}I_{2y}$. The evolution during period *B* is simply under the offset of spin 2

$$-2I_{1z}I_{2y} \xrightarrow{\Omega_2 t_1\ I_{2z}} -\cos\Omega_2 t_1\ 2I_{1z}I_{2y} + \sin\Omega_2 t_1\ 2I_{1z}I_{2x}$$

The next two 90° pulses transfer the first term to spin 1; the second term is rotated into multiple quantum and is not observed

$$-\cos\Omega_2 t_1\ 2I_{1z}I_{2y} + \sin\Omega_2 t_1\ 2I_{1z}I_{2x} \xrightarrow{\pi/2(I_{1x}+I_{2x})} -\cos\Omega_2 t_1\ 2I_{1y}I_{2z} - \sin\Omega_2 t_1\ 2I_{1y}I_{2x}$$

The first term on the right evolves during period *C* into in-phase magnetization (the evolution of offsets is refocused). So the final observable term is $\cos\Omega_2 t_1\ I_{1x}$. The resulting spectrum is therefore an in-phase doublet in F_2, centred at the offset of spin 1, and these peaks will both have the same frequency in F_1, namely the offset of spin 2. The spectrum looks just like the HMQC spectrum.

3.5 Multiple-quantum spectroscopy

A key feature of two-dimensional NMR experiments is that no direct observations are made during t_1, it is thus possible to detect, indirectly, the evolution of unobservable coherences. An example of the use of this feature is in the indirect detection of multiple-quantum spectra. A typical pulse sequence for such an experiment is shown opposite

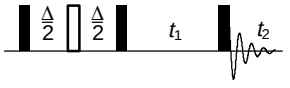

Pulse sequence for multiple-quantum spectroscopy.

For a two-spin system the optimum value for Δ is $1/(2J_{12})$. The sequence can be dissected as follows. The initial 90° – Δ/2 – 180° – Δ/2 – sequence is a spin echo which, at time Δ, refocuses any evolution of offsets but allows the coupling to evolve and generate anti-phase magnetization. This anti-phase magnetization is turned into multiple-quantum coherence by the second 90° pulse. After evolving for time t_1 the multiple quantum is returned into observable (anti-phase) magnetization by the final 90° pulse. Thus the first three pulses form the preparation period and the last pulse is

the mixing period.

3.5.1 Double-quantum spectrum for a three-spin system

The sequence will be analysed for a system of three spins. A complete analysis would be rather lengthy, so attention will be focused on certain terms as above, as many simplifying assumptions as possible will be made about the sequence.

The starting point will be equilibrium magnetization on spin 1, I_{1z}; after the spin echo the magnetization has evolved due to the coupling between spin 1 and spin 2, and the coupling between spin 1 and spin 3 (the 180° pulse causes an overall sign change (see section 2.4.1) but this has no real effect here so it will be ignored)

$$\begin{aligned} -I_{1y} &\xrightarrow{2\pi J_{12}\Delta I_{1z}I_{2z}} -\cos\pi J_{12}\Delta\ I_{1y} + \sin\pi J_{12}\Delta\ 2I_{1x}I_{2z} \\ &\xrightarrow{2\pi J_{13}\Delta I_{1z}I_{3z}} -\cos\pi J_{13}\Delta\ \cos\pi J_{12}\Delta\ I_{1y} + \sin\pi J_{13}\Delta\ \cos\pi J_{12}\Delta\ 2I_{1x}I_{3z} \\ &\qquad + \cos\pi J_{13}\Delta\ \sin\pi J_{12}\Delta\ 2I_{1x}I_{2z} + \sin\pi J_{13}\Delta\ \sin\pi J_{12}\Delta\ 4I_{1y}I_{2z}I_{3z} \end{aligned} \qquad [3.1]$$

Of these four terms, all but the first are turned into multiple-quantum by the second 90° pulse. For example, the second term becomes a mixture of double and zero quantum between spins 1 and 3

$$\sin\pi J_{13}\Delta\ \cos\pi J_{12}\Delta\ 2I_{1x}I_{3z} \xrightarrow{\pi/2\left(I_{1x}+I_{2x}+I_{3x}\right)} -\sin\pi J_{13}\Delta\ \cos\pi J_{12}\Delta\ 2I_{1x}I_{3y}$$

It will be assumed that appropriate coherence pathway selection (see section x.x) has been used so that ultimately only the double-quantum part contributes to the spectrum. This part is

$$\left[-\sin\pi J_{13}\Delta\ \cos\pi J_{12}\Delta\ \right]\left\{\tfrac{1}{2}\left(2I_{1x}I_{3y} + 2I_{1y}I_{3x}\right)\right\} \equiv B_{13}\mathrm{DQ}_y^{(13)}$$

The term in square brackets just gives the overall intensity, but does not affect the frequencies of the peaks in the two-dimensional spectrum as it does not depend on t_1 or t_2; this intensity term is denoted B_{13} for brevity. The operators in the curly brackets represent a pure double quantum state which can be denoted $\mathrm{DQ}_y^{(13)}$; the superscript (13) indicates that the double quantum is between spins 1 and 3 (see section 2.9).

As is shown in section 2.9, such a double-quantum term evolves under the offset according to

$$\begin{aligned} B_{13}\mathrm{DQ}_y^{(13)} &\xrightarrow{\Omega_1 t_1 I_{1z} + \Omega_2 t_1 I_{2z} + \Omega_3 t_1 I_{3z}} \\ &\qquad B_{13}\cos\left(\Omega_1 + \Omega_3\right)t_1\ \mathrm{DQ}_y^{(13)} - B_{13}\sin\left(\Omega_1 + \Omega_3\right)t_1\ \mathrm{DQ}_x^{(13)} \end{aligned}$$

where $\mathrm{DQ}_{\mathrm{x}}^{(13)} \equiv \frac{1}{2}\left(2I_{1x}I_{3x} - 2I_{1y}I_{3y}\right)$. This evolution is analogous to that of a single spin where *y* rotates towards *–x*.

As is also shown in section 2.9, $\mathrm{DQ}_y^{(13)}$ and $\mathrm{DQ}_x^{(13)}$ do not evolve under the coupling between spins 1 and 3, but they do evolve under the sum of the couplings between these two and all other spins; in this case this is simply $(J_{12}+J_{23})$. Taking each term in turn

$$B_{13}\cos\left(\Omega_1+\Omega_3\right)t_1\,\mathrm{DQ}_y^{(13)} \xrightarrow{2\pi J_{12}t_1 I_{1z}I_{2z}+2\pi J_{23}t_1 I_{2z}I_{3z}}$$
$$B_{13}\cos\left(\Omega_1+\Omega_3\right)t_1\cos\pi\left(J_{12}+J_{23}\right)t_1\,\mathrm{DQ}_y^{(13)}$$
$$-B_{13}\cos\left(\Omega_1+\Omega_3\right)t_1\sin\pi\left(J_{12}+J_{23}\right)t_1\,2I_{2z}\mathrm{DQ}_x^{(13)}$$
$$-B_{13}\sin\left(\Omega_1+\Omega_3\right)t_1\,\mathrm{DQ}_x^{(13)} \xrightarrow{2\pi J_{12}t_1 I_{1z}I_{2z}+2\pi J_{23}t_1 I_{2z}I_{3z}}$$
$$-B_{13}\sin\left(\Omega_1+\Omega_3\right)t_1\cos\pi\left(J_{12}+J_{23}\right)t_1\,\mathrm{DQ}_x^{(13)}$$
$$-B_{13}\sin\left(\Omega_1+\Omega_3\right)t_1\sin\pi\left(J_{12}+J_{23}\right)t_1\,2I_{2z}\mathrm{DQ}_y^{(13)}$$

Terms such as $2I_{2z}\mathrm{DQ}_y^{(13)}$ and $2I_{2z}\mathrm{DQ}_x^{(13)}$ can be thought of as double-quantum coherence which has become "anti-phase" with respect to the coupling to spin 2; such terms are directly analogous to single-quantum anti-phase magnetization.

Of all the terms present at the end of t_1, only $\mathrm{DQ}_y^{(13)}$ is rendered observable by the final pulse

$$\cos\left(\Omega_1+\Omega_3\right)t_1\cos\pi\left(J_{12}+J_{23}\right)t_1B_{13}\mathrm{DQ}_y^{(13)} \xrightarrow{\pi/2\left(I_{1x}+I_{2x}+I_{3x}\right)}$$
$$\cos\left(\Omega_1+\Omega_3\right)t_1\cos\pi\left(J_{12}+J_{23}\right)t_1B_{13}\left[2I_{1x}I_{3z}+2I_{1z}I_{3x}\right]$$

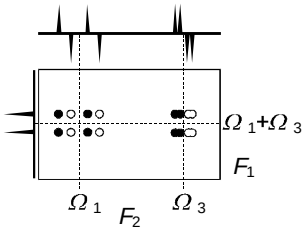

Schematic two-dimensional double quantum spectrum showing the multiplets arising from evolution of double-quantum coherence between spins 1 and 3. If has been assumed that $J_{12} > J_{13} > J_{23}$.

The calculation predicts that two two-dimensional multiplets appear in the spectrum. Both have the same structure in F_1, namely an in–phase doublet, split by $(J_{12} + J_{23})$ and centred at $(\Omega_1 + \Omega_3)$; this is analogous to a normal multiplet. In F_2 one two-dimensional multiplet is centred at the offset of spins 1, Ω_1, and one at the offset of spin 3, Ω_3; both multiplets are anti-phase with respect to the coupling J_{13}. Finally, the overall amplitude, B_{13}, depends on the delay Δ and all the couplings in the system. The schematic spectrum is shown opposite. Similar multiplet structures are seen for the double-quantum between spins 1 & 2 and spins 2 & 3.

3.5.2 Interpretation of double-quantum spectra

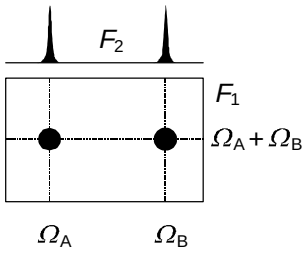

Schematic spectrum showing the relationship between the single- and double-quantum frequencies for coupled spins.

The double-quantum spectrum shows the relationship between the frequencies of the lines in the double quantum spectrum and those in the (conventional) single-quantum spectrum. If two two-dimensional multiplets appear at (F_1, F_2) = (Ω_A + Ω_B, Ω_A) and (Ω_A + Ω_B, Ω_B) the implication is that the two spins A and B are coupled, as it is only if there is a coupling present that double-quantum coherence between the two spins can be generated (e.g. in the previous section, if J_{13} = 0 the term B_{13}, goes to zero). The fact that the two two-dimensional multiplets share a common F_1 frequency and that this frequency is the sum of the two F_2 frequencies constitute a double check as to whether or not the peaks indicate that the spins are coupled.

Double quantum spectra give very similar information to that obtained from COSY i.e. the identification of coupled spins. Each method has particular advantages and disadvantages:

(1) In COSY the cross-peak multiplet is anti-phase in both dimensions, whereas in a double-quantum spectrum the multiplet is only anti-phase in F_2. This may lead to stronger peaks in the double-quantum spectrum due to less cancellation. However, during the two delays Δ magnetization is lost by relaxation, resulting in reduced peak intensities in the double-quantum spectrum.

(2) The value of the delay Δ in the double-quantum experiment affects the amount of multiple-quantum generated and hence the intensity in the spectrum. All of the couplings present in the spin system affect the intensity and as couplings cover a wide range, no single optimum value for Δ can be given. An unfortunate choice for Δ will result in low intensity, and it is then possible that correlations will be missed. No such problems occur with COSY.

(3) There are no diagonal-peak multiplets in a double-quantum spectrum, so that correlations between spins with similar offsets are relatively easy to locate. In contrast, in a COSY the cross-peaks from such a pair of spins could be obscured by the diagonal.

(4) In more complex spin systems the interpretation of a COSY remains unambiguous, but the double-quantum spectrum may show a peak with F_1 co-ordinate (Ω_A + Ω_B) and F_2 co-ordinate Ω_A (or Ω_B) even when spins A and B are not coupled. Such remote peaks, as they are called, appear when spins A and B are both coupled to a third spin. There are various tests that can differentiate these remote from the more useful direct peaks, but these require additional experiments. The form of these remote peaks in considered in the next section.

On the whole, COSY is regarded as a more reliable and simple experiment, although double-quantum spectroscopy is used in some special circumstances.

3.5.3 Remote peaks in double-quantum spectra

The origin of remote peaks can be illustrated by returning to the calculation of section 3.5.1. and focusing on the doubly anti-phase term which is present at the end of the spin echo (the fourth term in Eqn. [3.1])

$$\sin\pi J_{13}\Delta\ \sin\pi J_{12}\Delta\ 4I_{1y}I_{2z}I_{3z}$$

The 90° pulse rotates this into multiple-quantum

$$\sin\pi J_{13}\Delta\ \sin\pi J_{12}\Delta\ 4I_{1y}I_{2z}I_{3z} \xrightarrow{\pi/2\left(I_{1x}+I_{2x}+I_{3x}\right)} \sin\pi J_{13}\Delta\ \sin\pi J_{12}\Delta\ 4I_{1z}I_{2y}I_{3y}$$

The pure double-quantum part of this term is

$$-\tfrac{1}{2}\sin\pi J_{13}\Delta\ \sin\pi J_{12}\Delta\left(4I_{1z}I_{2x}I_{3x}-4I_{1z}I_{2y}I_{3y}\right)\equiv B_{23,1}2I_{1z}DQ_{x}^{(23)}$$

In words, what has been generated in double-quantum between spins 2 and 3, anti-phase with respect to spin 1. The key thing is that no coupling between spins 2 and 3 is required for the generation of this term – the intensity just depends on J_{12} and J_{13}; all that is required is that both spins 2 and 3 have a coupling to the third spin, spin 1.

During t_1 this term evolves under the influence of the offsets and the couplings. Only two terms ultimately lead to observable signals; at the end of t_1 these two terms are

$$B_{23,1}\cos\left(\Omega_2+\Omega_3\right)t_1\cos\pi\left(J_{12}+J_{13}\right)t_1\,2I_{1z}DQ_{x}^{(23)}$$
$$B_{23,1}\cos\left(\Omega_2+\Omega_3\right)t_1\sin\pi\left(J_{12}+J_{13}\right)t_1\,DQ_{y}^{(23)}$$

and after the final 90° pulse the observable parts are

$$B_{23,1}\cos\left(\Omega_2+\Omega_3\right)t_1\cos\pi\left(J_{12}+J_{13}\right)t_1\,4I_{1y}I_{2z}I_{3z}$$
$$B_{23,1}\cos\left(\Omega_2+\Omega_3\right)t_1\sin\pi\left(J_{12}+J_{13}\right)t_1\left(2I_{2x}I_{3z}+2I_{2z}I_{3x}\right)$$

The first term results in a multiplet appearing at Ω_1 in F_2 and at $(\Omega_2+\Omega_3)$ in F_1. The multiplet is doubly anti-phase (with respect to the couplings to spins 2 and 3) in F_2; in F_1 it is in-phase with respect to the sum of the couplings J_{12} and J_{13}. This multiplet is a remote peak, as its frequency coordinates do not conform to the simple pattern described in section 3.5.2. It is distinguished from direct peaks not only by its frequency coordinates, but also by having a different lineshape in F_2 to direct peaks and by being doubly anti-phase in that dimension.

The second and third terms are anti-phase with respect to the coupling between spins 2 and 3, and if this coupling is zero there will be cancellation within the multiplet and no signals will be observed. This is despite the fact that multiple-quantum coherence between these two spins has been generated.

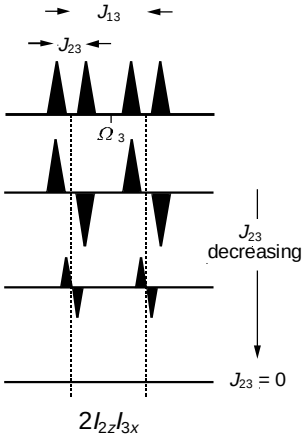

Illustration of how the intensity of an anti-phase multiplet decreases as the coupling which it is in anti-phase with respect to decreases. The in-phase multiplet is shown at the top, and below are three versions of the anti-phase multiplet for successively decreasing values of J_{23}.

3.6 Lineshapes and frequency discrimination

This is a somewhat involved topic which will only be possible to cover in outline in this lecture.

3.6.1 One-dimensional spectra

All modern spectrometers use a method know as quadrature detection, which in effect means that both the *x*- and *y*-components of the magnetization are detected simultaneously.

Suppose that a 90°(*y*) pulse is applied to equilibrium magnetization resulting in the generation of pure *x*-magnetization which then precesses in the transverse plane with frequency Ω. NMR spectrometers are set up to detect the *x*- and *y*-components of this magnetization. If it is assumed (arbitrarily) that these components decay exponentially with time constant T_2 the resulting signals, $S_x(t)$ and $S_y(t)$, from the two channels of the detector can be written

$$S_x(t) = \gamma \cos\Omega t \exp\left(-t/T_2\right) \quad S_y(t) = \gamma \sin\Omega t \exp\left(-t/T_2\right)$$

where γ is a factor which gives the absolute intensity of the signal.

Usually, these two components are combined in the computer to give a complex time-domain signal, $S(t)$

$$\begin{aligned} S(t) &= S_x(t) + iS_y(t) \\ &= \gamma\left(\cos\Omega t + i\sin\Omega t\right)\exp\left(-t/T_2\right) \\ &= \gamma \exp(i\Omega t)\exp\left(-t/T_2\right) \end{aligned} \qquad [3.2]$$

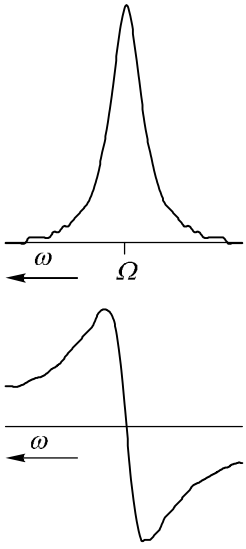

Absorption (above) and dispersion (below) Lorentzian lineshapes, centred at frequency Ω.

The Fourier transform of $S(t)$ is also a complex function, $S(\omega)$:

$$\begin{aligned} S(\omega) &= FT\left[S(t)\right] \\ &= \gamma\left\{A(\omega) + iD(\omega)\right\} \end{aligned}$$

where $A(\omega)$ and $D(\omega)$ are the absorption and dispersion Lorentzian lineshapes:

$$A(\omega) = \frac{1}{(\omega-\Omega)^2 T_2^2 + 1} \qquad D(\omega) = \frac{(\omega-\Omega)T_2}{(\omega-\Omega)^2 T_2^2 + 1}$$

These lineshapes are illustrated opposite. For NMR it is usual to display the spectrum with the absorption mode lineshape and in this case this corresponds to displaying the real part of $S(\omega)$.

3.6.1.1 Phase

Due to instrumental factors it is almost never the case that the real and

imaginary parts of $S(t)$ correspond exactly to the x- and y-components of the magnetization. Mathematically, this is expressed by multiplying the ideal function by an instrumental phase factor, ϕ_{instr}

$$S(t) = \gamma \exp\left(i\phi_{\text{instr}}\right) \exp(i\Omega t) \exp\left(-t/T_2\right)$$

The real and imaginary parts of $S(t)$ are

$$\begin{aligned}
\text{Re}\left[S(t)\right] &= \gamma\left(\cos\phi_{\text{instr}} \cos\Omega t - \sin\phi_{\text{instr}} \sin\Omega t\right) \exp\left(-t/T_2\right) \\
\text{Im}\left[S(t)\right] &= \gamma\left(\cos\phi_{\text{instr}} \sin\Omega t + \sin\phi_{\text{instr}} \cos\Omega t\right) \exp\left(-t/T_2\right)
\end{aligned}$$

Clearly, these do not correspond to the x– and y-components of the ideal time-domain function.

The Fourier transform of $S(t)$ carries forward the phase term

$$S(\omega) = \gamma \exp\left(i\phi_{\text{instr}}\right)\left\{A(\omega) + iD(\omega)\right\}$$

The real and imaginary parts of $S(\omega)$ are no longer the absorption and dispersion signals:

$$\begin{aligned}
\text{Re}\left[S(\omega)\right] &= \gamma\left(\cos\phi_{\text{instr}} A(\omega) - \sin\phi_{\text{instr}} D(\omega)\right) \\
\text{Im}\left[S(\omega)\right] &= \gamma\left(\cos\phi_{\text{instr}} D(\omega) + \sin\phi_{\text{instr}} A(\omega)\right)
\end{aligned}$$

Thus, displaying the real part of $S(\omega)$ will not give the required absorption mode spectrum; rather, the spectrum will show lines which have a mixture of absorption and dispersion lineshapes.

Restoring the pure absorption lineshape is simple. $S(\omega)$ is multiplied, in the computer, by a phase correction factor, ϕ_{corr}:

$$\begin{aligned}
S(\omega)\exp\left(i\phi_{\text{corr}}\right) &= \gamma \exp\left(i\phi_{\text{corr}}\right) \exp\left(i\phi_{\text{instr}}\right)\left\{A(\omega) + iD(\omega)\right\} \\
&= \gamma \exp\left(i\left(\phi_{\text{corr}} + \phi_{\text{instr}}\right)\right)\left\{A(\omega) + iD(\omega)\right\}
\end{aligned}$$

By choosing ϕ_{corr} such that $(\phi_{\text{corr}} + \phi_{\text{inst}}) = 0$ (*i.e.* $\phi_{\text{corr}} = -\phi_{\text{instr}}$) the phase terms disappear and the real part of the spectrum will have the required absorption lineshape. In practice, the value of the phase correction is set "by eye" until the spectrum "looks phased". NMR processing software also allows for an additional phase correction which depends on frequency; such a correction is needed to compensate for, amongst other things, imperfections in radiofrequency pulses.

3.6.1.2 Phase is arbitrary

Suppose that the phase of the 90° pulse is changed from *y* to *x*. The magnetization now starts along –*y* and precesses towards *x*; assuming that the instrumental phase is zero, the output of the two channels of the detector are

$$S_x(t) = \gamma \sin \Omega t \exp\left(-t/T_2\right) \quad S_y(t) = -\gamma \cos \Omega t \exp\left(-t/T_2\right)$$

The complex time-domain signal can then be written

$$\begin{aligned} S(t) &= S_x(t) + iS_y(t) \\ &= \gamma(\sin \Omega t - i \cos \Omega t) \exp\left(-t/T_2\right) \\ &\quad \gamma(-i)(\cos \Omega t + i \sin \Omega t) \exp\left(-t/T_2\right) \\ &= \gamma(-i) \exp(i\Omega t) \exp\left(-t/T_2\right) \\ &= \gamma \exp\left(i\phi_{\text{exp}}\right) \exp(i\Omega t) \exp\left(-t/T_2\right) \end{aligned}$$

Where ϕ_{exp}, the "experimental" phase, is $-\pi/2$ (recall that $\exp(i\phi) = \cos\phi + i \sin\phi$, so that $\exp(-i\,\pi/2) = -i$).

It is clear from the form of $S(t)$ that this phase introduced by altering the experiment (in this case, by altering the phase of the pulse) takes exactly the same form as the instrumental phase error. It can, therefore, be corrected by applying a phase correction so as to return the real part of the spectrum to the absorption mode lineshape. In this case the phase correction would be $\pi/2$.

The Fourier transform of the original signal is

$$\begin{gathered} S(\omega) = \gamma(-i)\{A(\omega) + iD(\omega)\} \\ \text{Re}[S(\omega)] = \gamma D(\omega) \qquad \text{Im}[S(\omega)] = -\gamma A(\omega) \end{gathered}$$

Thus the real part shows the dispersion mode lineshape, and the imaginary part shows the absorption lineshape. The 90° phase shift simply swaps over the real and imaginary parts.

3.6.1.3 Relative phase is important

The conclusion from the previous two sections is that the lineshape seen in the spectrum is under the control of the spectroscopist. It does not matter, for example, whether the pulse sequence results in magnetization appearing along the *x*- or *y*- axis (or anywhere in between, for that matter). It is always possible to phase correct the spectrum afterwards to achieve the desired lineshape.

However, if an experiment leads to magnetization from different processes or spins appearing along different axes, there is no single phase

correction which will put the whole spectrum in the absorption mode. This is the case in the COSY spectrum (section 3.4.1). The terms leading to diagonal-peaks appear along the *x*-axis, whereas those leading to cross-peaks appear along *y*. Either can be phased to absorption, but if one is in absorption, one will be in dispersion; the two signals are fundamentally 90° out of phase with one another.

3.6.1.4 Frequency discrimination

Suppose that a particular spectrometer is only capable of recording one, say the *x*-, component of the precessing magnetization. The time domain signal will then just have a real part (compare Eqn. [3.2] in section 3.6.1)

$$S(t) = \gamma \cos\Omega t \exp\left(-t/T_2\right)$$

Using the identity $\cos\theta = \frac{1}{2}\left(\exp(i\theta) + \exp(-i\theta)\right)$ this can be written

$$\begin{aligned} S(t) &= \tfrac{1}{2}\gamma\left[\exp(i\Omega t) + \exp(-i\Omega t)\right]\exp\left(-t/T_2\right) \\ &= \tfrac{1}{2}\gamma\exp(i\Omega t)\exp\left(-t/T_2\right) + \tfrac{1}{2}\gamma\exp(-i\Omega t)\exp\left(-t/T_2\right) \end{aligned}$$

The Fourier transform of the first term gives, in the real part, an absorption mode peak at $\omega = +\Omega$; the transform of the second term gives the same but at $\omega = -\Omega$.

$$\mathrm{Re}[S(\omega)] = \tfrac{1}{2}\gamma A_+ + \tfrac{1}{2}\gamma A_-$$

where A_+ represents an absorption mode Lorentzian line at $\omega = +\Omega$ and A_- represents the same at $\omega = -\Omega$; likewise, D_+ and D_- represent dispersion mode peaks at $+\Omega$ and $-\Omega$, respectively.

This spectrum is said to lack frequency discrimination, in the sense that it does not matter if the magnetization went round at $+\Omega$ or $-\Omega$, the spectrum still shows peaks at both $+\Omega$ and $-\Omega$. This is in contrast to the case where both the *x*- and *y*-components are measured where one peak appears at either positive or negative ω depending on the sign of Ω.

The lack of frequency discrimination is associated with the signal being modulated by a cosine wave, which has the property that $\cos(\Omega t) = \cos(-\Omega t)$, as opposed to a complex exponential, $\exp(i\Omega t)$ which is sensitive to the sign of Ω. In one-dimensional spectroscopy it is virtually always possible to arrange for the signal to have this desirable complex phase modulation, but in the case of two-dimensional spectra it is almost always the case that the signal modulation in the t_1 dimension is of the form $\cos(\Omega t_1)$ and so such spectra are not naturally frequency discriminated in the F_1 dimension.

Suppose now that only the *y*-component of the precessing magnetization could be detected. The time domain signal will then be (compare Eqn. [3.2] in section 3.6.1)

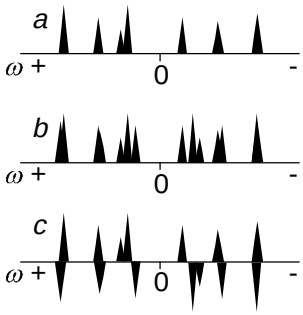

Spectrum *a* has peaks at positive and negative frequencies and is frequency discriminated. Spectrum *b* results from a cosine modulated time-domain data set; each peak appears at both positive and negative frequency, regardless of whether its real offset is positive or negative. Spectrum *c* results from a sine modulated data set; like *b* each peak appears twice, but with the added complication that one peak is inverted. Spectra *b* and *c* lack frequency discrimination and are quite uninterpretable as a result.

$$S(t) = i\gamma \sin \Omega t \exp\left(-t/T_2\right)$$

Using the identity $\sin\theta = \frac{1}{2i}\left(\exp(i\theta) - \exp(-i\theta)\right)$ this can be written

$$\begin{aligned} S(t) &= \tfrac{1}{2}\gamma\left[\exp(i\Omega t) - \exp(-i\Omega t)\right]\exp\left(-t/T_2\right) \\ &= \tfrac{1}{2}\gamma \exp(i\Omega t)\exp\left(-t/T_2\right) - \tfrac{1}{2}\gamma \exp(-i\Omega t)\exp\left(-t/T_2\right) \end{aligned}$$

and so

$$\mathrm{Re}[S(\omega)] = \tfrac{1}{2}\gamma A_+ - \tfrac{1}{2}\gamma A_-$$

This spectrum again shows two peaks, at $\pm\Omega$, but the two peaks have opposite signs; this is associated with the signal being modulated by a sine wave, which has the property that $\sin(-\Omega t) = -\sin(\Omega t)$. If the sign of Ω changes the two peaks swap over, but there are still two peaks. In a sense the spectrum is frequency discriminated, as positive and negative frequencies can be distinguished, but in practice in a spectrum with many lines with a range of positive and negative offsets the resulting set of possibly cancelling peaks would be impossible to sort out satisfactorily.

3.6.2 Two-dimensional spectra

3.6.2.1 Phase and amplitude modulation

There are two basic types of time-domain signal that are found in two-dimensional experiments. The first is phase modulation, in which the evolution in t_1 is encoded as a phase, *i.e.* mathematically as a complex exponential

$$S\left(t_1, t_2\right)_{\text{phase}} = \gamma \exp\left(i\Omega_1 t_1\right)\exp\left(-t_1/T_2^{(1)}\right)\exp\left(i\Omega_2 t_2\right)\exp\left(-t_2/T_2^{(2)}\right)$$

where Ω_1 and Ω_2 are the modulation frequencies in t_1 and t_2 respectively, and $T_2^{(1)}$ and $T_2^{(2)}$ are the decay time constants in t_1 and t_2 respectively.

The second type is amplitude modulation, in which the evolution in t_1 is encoded as an amplitude, *i.e.* mathematically as sine or cosine

$$\begin{aligned} S(t)_c &= \gamma \cos\left(\Omega_1 t_1\right)\exp\left(-t_1/T_2^{(1)}\right)\exp\left(i\Omega_2 t_2\right)\exp\left(-t_2/T_2^{(2)}\right) \\ S(t)_s &= \gamma \sin\left(\Omega_1 t_1\right)\exp\left(-t_1/T_2^{(1)}\right)\exp\left(i\Omega_2 t_2\right)\exp\left(-t_2/T_2^{(2)}\right) \end{aligned}$$

Generally, two-dimensional experiments produce amplitude modulation, indeed all of the experiments analysed in this chapter have produced either sine or cosine modulated data. Therefore most two-dimensional spectra are

fundamentally not frequency discriminated in the F_1 dimension. As explained above for one-dimensional spectra, the resulting confusion in the spectrum is not acceptable and steps have to be taken to introduce frequency discrimination.

It will turn out that the key to obtaining frequency discrimination is the ability to record, in separate experiments, both sine and cosine modulated data sets. This can be achieved by simply altering the phase of the pulses in the sequence.

For example, consider the EXSY sequence analysed in section 3.2 . The observable signal, at time $t_2 = 0$, can be written

$$(1-f)\cos\Omega_1 t_1 \; I_{1y} + f\cos\Omega_1 t_1 \; I_{2y}$$

If, however, the first pulse in the sequence is changed in phase from *x* to *y* the corresponding signal will be

$$-(1-f)\sin\Omega_1 t_1 \; I_{1y} - f\sin\Omega_1 t_1 \; I_{2y}$$

i.e. the modulation has changed from the form of a cosine to sine. In COSY and DQF COSY a similar change can be brought about by altering the phase of the first 90° pulse. In fact there is a general procedure for effecting this change, the details of which are given in lecture 4.

3.6.2.2 Two-dimensional lineshapes

The spectra resulting from two-dimensional Fourier transformation of phase and amplitude modulated data sets can be determined by using the following Fourier pair

$$FT\left[\exp(i\Omega t)\exp\left(-t/T_2\right)\right] = \{A(\omega) + iD(\omega)\}$$

where *A* and *D* are the dispersion Lorentzian lineshapes described in section 3.6.1

Phase modulation

For the phase modulated data set the transform with respect to t_2 gives

$$S\left(t_1,\omega_2\right)_{\text{phase}} = \gamma\exp\left(i\Omega_1 t_1\right)\exp\left(-t_1/T_2^{(1)}\right)\left[A_+^{(2)} + iD_+^{(2)}\right]$$

where $A_+^{(2)}$ indicates an absorption mode line in the F_2 dimension at $\omega_2 = +\Omega_2$ and with linewidth set by $T_2^{(2)}$; similarly $D_+^{(2)}$ is the corresponding dispersion line.

The second transform with respect to t_1 gives

$$S(\omega_1,\omega_2)_{\text{phase}} = \gamma\left[A_+^{(1)} + iD_+^{(1)}\right]\left[A_+^{(2)} + iD_+^{(2)}\right]$$

where $A_+^{(1)}$ indicates an absorption mode line in the F_1 dimension at $\omega_1 = +\Omega_1$ and with linewidth set by $T_2^{(1)}$; similarly $D_+^{(1)}$ is the corresponding dispersion line.

The real part of the resulting two-dimensional spectrum is

$$\text{Re}\left[S(\omega_1,\omega_2)_{\text{phase}}\right] = \gamma\left(A_+^{(1)}A_+^{(2)} - D_+^{(1)}D_+^{(2)}\right)$$

This is a single line at $(\omega_1,\omega_2) = (+\Omega_1,+\Omega_2)$ with the phase-twist lineshape, illustrated below.

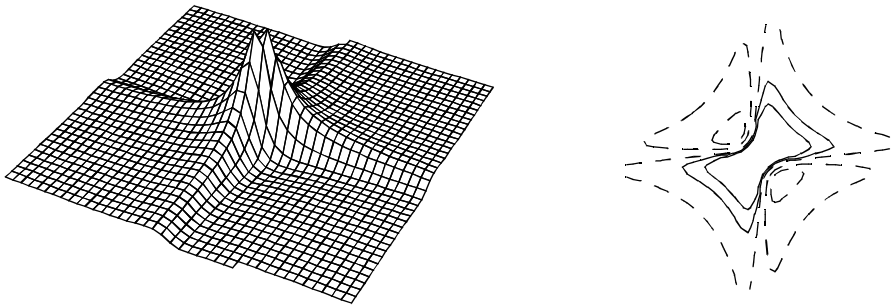

Pseudo 3D view and contour plot of the phase-twist lineshape.

The phase-twist lineshape is an inextricable mixture of absorption and dispersion; it is a superposition of the double absorption and double dispersion lineshape (illustrated in section 3.4.1). No phase correction will restore it to pure absorption mode. Generally the phase twist is not a very desirable lineshape as it has both positive and negative parts, and the dispersion component only dies off slowly.

Cosine amplitude modulation

For the cosine modulated data set the transform with respect to t_2 gives

$$S(t_1,\omega_2)_c = \gamma\cos(\Omega_1 t_1)\exp\left(-t_1/T_2^{(1)}\right)\left[A_+^{(2)} + iD_+^{(2)}\right]$$

The cosine is then rewritten in terms of complex exponentials to give

$$S(t_1,\omega_2)_c = \tfrac{1}{2}\gamma\left[\exp(i\Omega_1 t_1) + \exp(-i\Omega_1 t_1)\right]\exp\left(-t_1/T_2^{(1)}\right)\left[A_+^{(2)} + iD_+^{(2)}\right]$$

The second transform with respect to t_1 gives

$$S(\omega_1,\omega_2)_c = \tfrac{1}{2}\gamma\left[\left\{A_+^{(1)} + iD_+^{(1)}\right\} + \left\{A_-^{(1)} + iD_-^{(1)}\right\}\right]\left[A_+^{(2)} + iD_+^{(2)}\right]$$

where $A_-^{(1)}$ indicates an absorption mode line in the F_1 dimension at $\omega_1 = -\Omega_1$ and with linewidth set by $T_2^{(1)}$; similarly $D_-^{(1)}$ is the corresponding dispersion line.

The real part of the resulting two-dimensional spectrum is

$$\mathrm{Re}\left[S(\omega_1,\omega_2)_c\right] = \tfrac{1}{2}\gamma\left(A_+^{(1)}A_+^{(2)} - D_+^{(1)}D_+^{(2)}\right) + \tfrac{1}{2}\gamma\left(A_-^{(1)}A_+^{(2)} - D_-^{(1)}D_+^{(2)}\right)$$

This is a two lines, both with the phase-twist lineshape; one is located at $(+\Omega_1,+\Omega_2)$ and the other is at $(-\Omega_1,+\Omega_2)$. As expected for a data set which is cosine modulated in t_1 the spectrum is symmetrical about $\omega_1 = 0$.

A spectrum with a pure absorption mode lineshape can be obtained by discarding the imaginary part of the time domain data immediately after the transform with respect to t_2; *i.e.* taking the real part of $S(t_1,\omega_2)_c$

$$\begin{aligned} S(t_1,\omega_2)_c^{\mathrm{Re}} &= \mathrm{Re}\left[S(t_1,\omega_2)_c\right] \\ &= \gamma\cos(\Omega_1 t_1)\exp\left(-t_1/T_2^{(1)}\right)A_+^{(2)} \end{aligned}$$

Following through the same procedure as above:

$$S(t_1,\omega_2)_c^{\mathrm{Re}} = \tfrac{1}{2}\gamma\left[\exp(i\Omega_1 t_1) + \exp(-i\Omega_1 t_1)\right]\exp\left(-t_1/T_2^{(1)}\right)A_+^{(2)}$$

$$S(\omega_1,\omega_2)_c^{\mathrm{Re}} = \tfrac{1}{2}\gamma\left[\left\{A_+^{(1)} + iD_+^{(1)}\right\} + \left\{A_-^{(1)} + iD_-^{(1)}\right\}\right]A_+^{(2)}$$

The real part of the resulting two-dimensional spectrum is

$$\mathrm{Re}\left[S(\omega_1,\omega_2)_c^{\mathrm{Re}}\right] = \tfrac{1}{2}\gamma A_+^{(1)}A_+^{(2)} + \tfrac{1}{2}\gamma A_-^{(1)}A_+^{(2)}$$

This is two lines, located at $(+\Omega_1,+\Omega_2)$ and $(-\Omega_1,+\Omega_2)$, but in contrast to the above both have the double absorption lineshape. There is still lack of frequency discrimination, but the undesirable phase-twist lineshape has been avoided.

Sine amplitude modulation

For the sine modulated data set the transform with respect to t_2 gives

$$S(t_1,\omega_2)_s = \gamma \sin(\Omega_1 t_1)\exp(-t_1/T_2^{(1)})\left[A_+^{(2)} + iD_+^{(2)}\right]$$

The cosine is then rewritten in terms of complex exponentials to give

$$S(t_1,\omega_2)_s = \tfrac{1}{2i}\gamma\left[\exp(i\Omega_1 t_1) - \exp(-i\Omega_1 t_1)\right]\exp(-t_1/T_2^{(1)})\left[A_+^{(2)} + iD_+^{(2)}\right]$$

The second transform with respect to t_1 gives

$$S(\omega_1,\omega_2)_s = \tfrac{1}{2i}\gamma\left[\left\{A_+^{(1)} + iD_+^{(1)}\right\} - \left\{A_-^{(1)} + iD_-^{(1)}\right\}\right]\left[A_+^{(2)} + iD_+^{(2)}\right]$$

The imaginary part of the resulting two-dimensional spectrum is

$$\mathrm{Im}\left[S(\omega_1,\omega_2)_s\right] = -\tfrac{1}{2}\gamma\left(A_+^{(1)}A_+^{(2)} - D_+^{(1)}D_+^{(2)}\right) + \tfrac{1}{2}\gamma\left(A_-^{(1)}A_+^{(2)} - D_-^{(1)}D_+^{(2)}\right)$$

This is two lines, both with the phase-twist lineshape but with opposite signs; one is located at $(+\Omega_1,+\Omega_2)$ and the other is at $(-\Omega_1,+\Omega_2)$. As expected for a data set which is sine modulated in t_1 the spectrum is anti-symmetric about $\omega_1 = 0$.

As before, a spectrum with a pure absorption mode lineshape can be obtained by discarding the imaginary part of the time domain data immediately after the transform with respect to t_2; *i.e.* taking the real part of $S(t_1,\omega_2)_s$

$$\begin{aligned} S(t_1,\omega_2)_s^{\mathrm{Re}} &= \mathrm{Re}\left[S(t_1,\omega_2)_s\right] \\ &= \gamma \sin(\Omega_1 t_1)\exp(-t_1/T_2^{(1)})A_+^{(2)} \end{aligned}$$

Following through the same procedure as above:

$$S(t_1,\omega_2)_s^{\mathrm{Re}} = \tfrac{1}{2i}\gamma\left[\exp(i\Omega_1 t_1) - \exp(-i\Omega_1 t_1)\right]\exp(-t_1/T_2^{(1)})A_+^{(2)}$$

$$S(\omega_1,\omega_2)_s^{\mathrm{Re}} = \tfrac{1}{2i}\gamma\left[\left\{A_+^{(1)} + iD_+^{(1)}\right\} - \left\{A_-^{(1)} + iD_-^{(1)}\right\}\right]A_+^{(2)}$$

The imaginary part of the resulting two-dimensional spectrum is

$$\mathrm{Im}\left[S(\omega_1,\omega_2)_s^{\mathrm{Re}}\right] = -\tfrac{1}{2}\gamma A_+^{(1)}A_+^{(2)} + \tfrac{1}{2}\gamma A_-^{(1)}A_+^{(2)}$$

The two lines now have the pure absorption lineshape.

3.6.2.3 Frequency discrimination with retention of absorption lineshapes

It is essential to be able to combine frequency discrimination in the F_1 dimension with retention of pure absorption lineshapes. Three different ways of achieving this are commonly used; each will be analysed here.

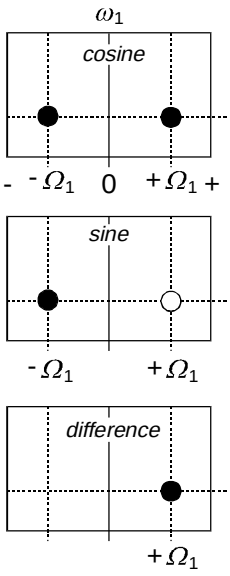

Illustration of the way in which the SHR method achieves frequency discrimination by combining cosine and sine modulated spectra.

States-Haberkorn-Ruben method

The essence of the States-Haberkorn-Ruben (SHR) method is the observation that the cosine modulated data set, processed as described in section 3.6.2.2, gives two positive absorption mode peaks at ($+\Omega_1$,$+\Omega_2$) and ($-\Omega_1$,$+\Omega_2$), whereas the sine modulated data set processed in the same way gives a spectrum in which one peak is negative and one positive. Subtracting these spectra from one another gives the required absorption mode frequency discriminated spectrum (see the diagram below):

$$\begin{aligned}\mathrm{Re}\left[S(\omega_1,\omega_2)_{\mathrm{c}}^{\mathrm{Re}}\right]-\mathrm{Im}\left[S(\omega_1,\omega_2)_{\mathrm{s}}^{\mathrm{Re}}\right]&\\ =\left[\tfrac{1}{2}\gamma A_+^{(1)}A_+^{(2)}+\tfrac{1}{2}\gamma A_-^{(1)}A_+^{(2)}\right]-\left[-\tfrac{1}{2}\gamma A_+^{(1)}A_+^{(2)}+\tfrac{1}{2}\gamma A_-^{(1)}A_+^{(2)}\right]&\\ =\gamma A_+^{(1)}A_+^{(2)}&\end{aligned}$$

In practice it is usually more convenient to achieve this result in the following way, which is mathematically identical.

The cosine and sine data sets are transformed with respect to t_2 and the real parts of each are taken. Then a new complex data set is formed using the cosine data for the real part and the sine data for the imaginary part:

$$\begin{aligned}S(t_1,\omega_2)_{\mathrm{SHR}}&=S(t_1,\omega_2)_{\mathrm{c}}^{\mathrm{Re}}+iS(t_1,\omega_2)_{\mathrm{s}}^{\mathrm{Re}}\\ &=\gamma\cos(\Omega_1 t_1)\exp\left(-t_1/T_2^{(1)}\right)A_+^{(2)}+i\gamma\sin(\Omega_1 t_1)\exp\left(-t_1/T_2^{(1)}\right)A_+^{(2)}\\ &=\gamma\exp(i\Omega_1 t_1)\exp\left(-t_1/T_2^{(1)}\right)A_+^{(2)}\end{aligned}$$

Fourier transformation with respect to t_1 gives a spectrum whose real part contains the required frequency discriminated absorption mode spectrum

$$\begin{aligned}S(\omega_1,\omega_2)_{\mathrm{SHR}}&=\gamma\left[A_+^{(1)}+iD_+^{(1)}\right]A_+^{(2)}\\ &=\gamma A_+^{(1)}A_+^{(2)}+iD_+^{(1)}A_+^{(2)}\end{aligned}$$

Marion-Wüthrich or TPPI method

The idea behind the TPPI (time proportional phase incrementation) or Marion–Wüthrich (MW) method is to arrange things so that all of the peaks have positive offsets. Then, frequency discrimination would not be required as there would be no ambiguity.

One simple way to make all offsets positive is to set the receiver carrier frequency deliberately at the edge of the spectrum. Simple though this is, it is not really a very practical method as the resulting spectrum would be very inefficient in its use of data space and in addition off-resonance effects associated with the pulses in the sequence will be accentuated.

In the TPPI method the carrier can still be set in the middle of the spectrum, but it is made to appear that all the frequencies are positive by phase shifting systematically some of the pulses in the sequence in concert with the incrementation of t_1.

In section 3.2 it was shown that in the EXSY sequence the cosine modulation in t_1, $\cos(\Omega_1 t_1)$, could be turned into sine modulation, $-\sin(\Omega_1 t_1)$, by shifting the phase of the first pulse by 90°. The effect of such a phase shift can be represented mathematically in the following way.

Recall that Ω is in units of radians s^{-1}, and so if t is in seconds Ωt is in radians; Ωt can therefore be described as a phase which depends on time. It is also possible to consider phases which do not depend on time, as was the case for the phase errors considered in section 3.6.1.1

The change from cosine to sine modulation in the EXSY experiment can be though of as a phase shift of the signal in t_1. Mathematically, such a phase shifted cosine wave is written as $\cos(\Omega_1 t_1 + \phi)$, where ϕ is the phase shift in radians. This expression can be expanded using the well known formula $\cos(A + B) = \cos A \cos B - \sin A \sin B$ to give

$$\cos\left(\Omega_1 t_1 + \phi\right) = \cos\Omega_1 t \cos\phi - \sin\Omega_1 t \sin\phi$$

If the phase shift, ϕ, is $\pi/2$ radians the result is

$$\begin{aligned}\cos\left(\Omega_1 t_1 + \pi/2\right) &= \cos\Omega_1 t \cos\pi/2 - \sin\Omega_1 t \sin\pi/2 \\ &= -\sin\Omega_1 t\end{aligned}$$

In words, a cosine wave, phase shifted by $\pi/2$ radians (90°) is the same thing as a sine wave. Thus, in the EXSY experiment the effect of changing the phase of the first pulse by 90° can be described as a phase shift of the signal by 90°.

Suppose that instead of a fixed phase shift, the phase shift is made proportional to t_1; what this means is that each time t_1 is incremented the phase is also incremented in concert. The constant of proportion between the time dependent phase, $\phi(t_1)$, and t_1 will be written $\omega_{\text{additional}}$

$$\phi\left(t_1\right) = \omega_{\text{additional}} t_1$$

Clearly the units of $\omega_{\text{additional}}$ are radians s^{-1}, that is $\omega_{\text{additional}}$ is a frequency. The new time-domain function with the inclusion of this incrementing phase is thus

$$\begin{aligned}\cos\left(\Omega_1 t_1 + \phi(t_1)\right) &= \cos\left(\Omega_1 t_1 + \omega_{\text{additional}} t_1\right) \\ &= \cos\left(\Omega_1 + \omega_{\text{additional}}\right) t_1\end{aligned}$$

In words, the effect of incrementing the phase in concert with t_1 is to add a frequency $\omega_{\text{additional}}$ to all of the offsets in the spectrum. The TPPI method utilizes this option of shifting all the frequencies in the following way.

In one-dimensional pulse-Fourier transform NMR the free induction signal is sampled at regular intervals Δ. After transformation the resulting spectrum displays correctly peaks with offsets in the range –(SW/2) to +(SW/2) where SW is the spectral width which is given by $1/\Delta$ (this comes about from the Nyquist theorem of data sampling). Frequencies outside this range are not represented correctly.

Suppose that the required frequency range in the F_1 dimension is from –(SW_1/2) to +(SW_1/2) (in COSY and EXSY this will be the same as the range in F_2). To make it appear that all the peaks have a positive offset, it will be necessary to add (SW_1/2) to all the frequencies. Then the peaks will be in the range 0 to (SW_1).

As the maximum frequency is now (SW_1) rather than (SW_1/2) the sampling interval, Δ_1, will have to be halved *i.e.* $\Delta_1 = 1/(2SW_1)$ in order that the range of frequencies present are represented properly.

The phase increment is $\omega_{\text{additional}} t_1$, but t_1 can be written as $n\Delta_1$ for the nth increment of t_1. The required value for $\omega_{\text{additional}}$ is $2\pi(SW_1/2)$, where the 2π is to convert from frequency (the units of SW_1) to rad s^{-1}, the units of $\omega_{\text{additional}}$. Putting all of this together $\omega_{\text{additional}} t_1$ can be expressed, for the nth increment as

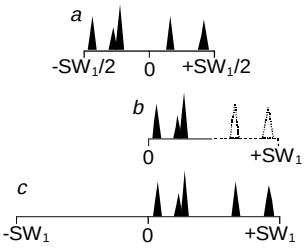

Illustration of the TPPI method. The normal spectrum is shown in *a*, with peaks in the range –SW/2 to +SW/2. Adding a frequency of SW/2 to all the peaks gives them all positive offsets, but some, shown dotted) will then fall outside the spectral window – spectrum *b*. If the spectral width is doubled all peaks are represented correctly – spectrum *c*.

$$\begin{aligned}\omega_{\text{additional}} t_1 &= 2\pi\left(\frac{SW_1}{2}\right)\left(n\Delta_1\right) \\ &= 2\pi\left(\frac{SW_1}{2}\right)\left(n\frac{1}{2SW_1}\right) \\ &= n\frac{\pi}{2}\end{aligned}$$

The way in which the phase incrementation increases the frequency of the cosine wave is shown below:

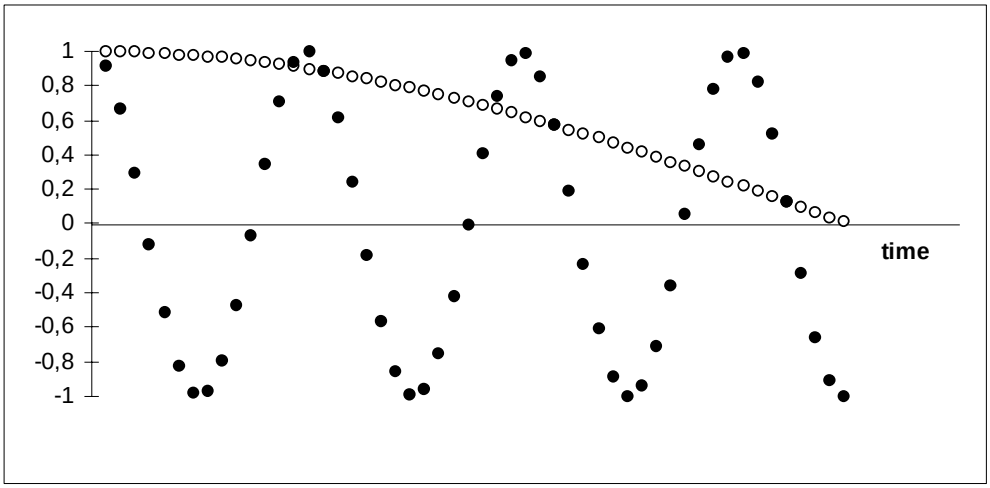

The open circles lie on a cosine wave, $\cos(\Omega \times n\Delta)$, where Δ is the sampling interval and n runs 0, 1, 2 ... The closed circles lie on a cosine wave in which an additional phase is incremented on each point i.e. the function is $\cos(\Omega \times n\Delta + n\phi)$; here $\phi = \pi/8$. The way in which this phase increment increases the frequency of the cosine wave is apparent.

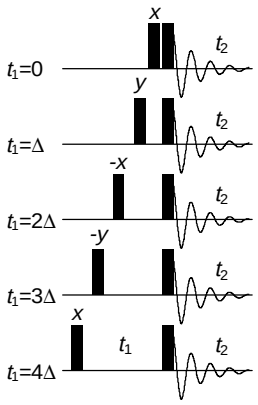

TPPI phase incrementation applied to a COSY sequence. The phase of the first pulse is incremented by 90° each time t_1 is incremented.

In words this means that each time t_1 is incremented, the phase of the signal should also be incremented by 90°, for example by incrementing the phase of one of the pulses. The way in which it can be decided which pulse to increment will be described in lecture 4.

A data set from an experiment to which TPPI has been applied is simply amplitude modulated in t_1 and so can be processed according to the method described for cosine modulated data so as to obtain absorption mode lineshapes. As the spectrum is symmetrical about $F_1 = 0$ it is usual to use a modified Fourier transform routine which saves effort and space by only calculating the positive frequency part of the spectrum.

Echo anti-echo method

Few two-dimensional experiments naturally produce phase modulated data sets, but if gradient pulses are used for coherence pathway selection (see lecture 4) it is then quite often found that the data are phase modulated. In one way this is an advantage, as it means that no special steps are required to obtain frequency discrimination. However, phase modulated data sets give rise to spectra with phase-twist lineshapes, which are very undesirable. So, it is usual to attempt to use some method to eliminate the phase-twist lineshape, while at the same time retaining frequency discrimination.

The key to how this can be done lies in the fact that two kinds of phase modulated data sets can usually be recorded. The first is called the *P*-type or anti-echo spectrum

$$S(t_1,t_2)_{\mathrm{p}} = \gamma \exp(i\Omega_1 t_1)\exp\left(-t_1/T_2^{(1)}\right)\exp(i\Omega_2 t_2)\exp\left(-t_2/T_2^{(2)}\right)$$

the "*P*" indicates positive, meaning here that the sign of the frequencies in F_1 and F_2 are the same.

The second data set is called the echo or *N*-type

$$S(t_1,t_2)_{\mathrm{N}} = \gamma \exp(-i\Omega_1 t_1)\exp\left(-t_1/T_2^{(1)}\right)\exp(i\Omega_2 t_2)\exp\left(-t_2/T_2^{(2)}\right)$$

the "*N*" indicates negative, meaning here that the sign of the frequencies in F_1 and F_2 are opposite. As will be explained in lecture 4 in gradient experiments it is easy to arrange to record either the *P*- or *N*-type spectrum.

The simplest was to proceed is to compute two new data sets which are

$$\begin{aligned}
&\tfrac{1}{2}\left[S(t_1,t_2)_{\mathrm{P}} + S(t_1,t_2)_{\mathrm{N}}\right] = \\
&\quad \tfrac{1}{2}\gamma\left[\exp(i\Omega_1 t_1) + \exp(-i\Omega_1 t_1)\right]\exp\left(-t_1/T_2^{(1)}\right)\exp(i\Omega_2 t_2)\exp\left(-t_2/T_2^{(2)}\right) \\
&\quad = \gamma\cos(\Omega_1 t_1)\exp\left(-t_1/T_2^{(1)}\right)\exp(i\Omega_2 t_2)\exp\left(-t_2/T_2^{(2)}\right)
\end{aligned}$$

$$\begin{aligned}
&\tfrac{1}{2i}\left[S(t_1,t_2)_{\mathrm{P}} - S(t_1,t_2)_{\mathrm{N}}\right] = \\
&\quad \tfrac{1}{2i}\gamma\left[\exp(i\Omega_1 t_1) - \exp(-i\Omega_1 t_1)\right]\exp\left(-t_1/T_2^{(1)}\right)\exp(i\Omega_2 t_2)\exp\left(-t_2/T_2^{(2)}\right) \\
&\quad = \gamma\sin(\Omega_1 t_1)\exp\left(-t_1/T_2^{(1)}\right)\exp(i\Omega_2 t_2)\exp\left(-t_2/T_2^{(2)}\right)
\end{aligned}$$

These two combinations are just the cosine and sine modulated data sets that are the inputs needed for the SHR method. The pure absorption spectrum can therefore be calculated in the same way starting with these combinations.

3.6.2.4 Phase in two-dimensional spectra

In practice there will be instrumental and other phase shifts, possibly in both dimensions, which mean that the time-domain functions are not the idealised ones treated above. For example, the cosine modulated data set might be

$$S(t)_c = \gamma\cos(\Omega_1 t_1 + \phi_1)\exp\left(-t_1/T_2^{(1)}\right)\exp(i\Omega_2 t_2 + i\phi_2)\exp\left(-t_2/T_2^{(2)}\right)$$

where ϕ_1 and ϕ_2 are the phase errors in F_1 and F_1, respectively. Processing this data set in the manner described above will not give a pure absorption spectrum. However, it is possible to recover the pure absorption spectrum by software manipulations of the spectrum, just as was described for the case of one-dimensional spectra. Usually, NMR data processing software provides options for making such phase corrections to two-dimensional data sets.